Functional Connectivity in Adolescents with Autism Spectrum Disorders

by

Samantha Ashinoff

A Thesis Submitted in Partial Fulfillment of the

Requirements for the Degree of Bachelor of Science

With Honors in BBCS from the

University of Michigan

2011

Advisor: Dr. Christopher Monk

Abstract

Atypical functional connectivity patterns are thought to play a role in the social impairment that is characteristic of autism spectrum disorders (ASD). This is an fMRI study of the default network and the amygdala-ventromedial prefrontal cortex (vmPFC) pathway, both of which play a role in social processing. Functional connectivity of these structures was examined in the presence of social stimuli versus during rest, in adolescents with ASD versus typically developing adolescents. As compared to controls, there was a trend of underconnectivity in the default network in ASD during the faces task, similar to the underconnectivity found in ASD during rest. There was also weaker posterior default network to left superior frontal gyrus (lSFG) connectivity during social processing than during rest, exclusively in the ASD group. These results may suggest intrinsically altered default network functioning in ASD. Due to technical limitations during amygdala-vmPFC analyses, these results remain unknown.

Functional Connectivity in Adolescents with Autism Spectrum Disorders

Autism spectrum disorders (ASD) are neurodevelopmental syndromes defined by deficits in social functioning and communication as well as repetitive and restricted behaviors and/or interests (APA, 1994). Both structural and functional evidence suggest that ASD is a disorder of atypical connectivity among brain structures (Belmonte et al., 2004). Functional connectivity is defined as the temporal correlation of neurophysiological events in spatially distinct brain regions (Friston, Frith, Liddle, & Frackowiak, 1993). Thus, atypical functional connectivity refers to a significantly increased or decreased statistical correlation of activity between particular brain regions than is found in healthy control populations. Atypical connectivity patterns have emerged in ASD in two networks involved in social processing: the default network and the amygdala-ventromedial prefrontal cortex.

Default Network

The default network is comprised of the posterior cingulate cortex (PCC), precuneus, retrosplenial, lateral parietal gyrus, superior temporal gyrus, medial prefrontal cortex, superior frontal gyrus, and parahippocampal gyrus (Buckner, Andrews-Hanna, & Schacter, 2008; Fox et al., 2005; Greicius, Krasnow, Reiss, & Menon, 2003). This group of brain structures activates when an individual is not involved in a demanding cognitive task, or during "rest" (Buckner et al., 2008). Though the primary function of the default network is still under debate, structures within this network are also active during social tasks related to the self, self-projection, and mentalizing (Buckner & Carroll, 2007; Frith & Frith, 2003; Gusnard & Raichle, 2001). Thus, it appears that the default network plays a role in social cognition and theory of mind, which refer to one's ability to understand and predict the emotions and actions of others. Deficits in social cognition and theory of mind may underlie the social impairment that is characteristic of ASD (Baron-Cohen et al., 1994). In particular, it has been theorized that individuals with ASD who

have difficulty thinking about what others are thinking may miss key developmental opportunities to learn and practice appropriate social responses to others. Therefore, networks relevant to social cognition, particularly the default network, have recently been the subject of increased scientific interest in relation to ASD.

Several studies have implicated altered default network functioning in ASD. During rest, adolescents with ASD show widespread weaker connectivity of default network structures compared to controls (Weng et al., 2010), as do adults (Monk et al., 2009). Notably, connectivity from the posterior portion of the default network to the right superior frontal gyrus is significantly diminished during rest in adolescents with ASD compared to controls (Weng et al., 2010; Wiggins et al., 2011). It has also been shown that weaker default network connectivity is correlated with poorer social functioning (Weng et al., 2010). However, whether or not this altered connectivity of the default network persists during the presence of social stimuli for individuals with ASD is still unclear. During rest, the observed underconnectivity may be explained as a function of the types of cognition underwent by participants as their minds wandered, namely social versus non-social. If the default network is underconnected during social processing as well as rest, this would indicate widespread, fundamentally abnormal functioning of the network structures. The first objective of this study was to examine default network connectivity during socio-emotional stimulation, in adolescents with ASD versus typically developing adolescents.

Amygdala-vmPFC

Another network of interest in ASD is the amygdala-ventromedial prefrontal cortex (vmPFC) circuit. The amygdala and ventromedial prefrontal cortex are structures responsive to socio-emotional information. They form a pathway that is thought to be key in emotional

processing, which is impaired in individuals with ASD (APA, 1994). Although some studies have found weaker connectivity in the amygdala-vmPFC circuit (Ashwin, Baron-Cohen, Wheelwright, O'Riordan, & Bullmore, 2007; Hadjikhani, Joseph, Snyder, & Tager-Flusberg, 2007), when controlling for attention, adults with ASD have shown stronger connectivity of this network in response to emotional faces than controls (Monk et al., 2010; Weng et al., 2011). This suggests that individuals with ASD may be paying less attention to emotional faces, possibly because they find the faces aversive or less socially rewarding. Reduced attention to faces is consistent with clinical reports of decreased eye contact with others (APA, 1994). Additionally, increased amygdala activation is linked to more severe social symptoms in ASD (Monk et al., 2010). While evidence clearly indicates increased amygdala-vmPFC connectivity during social tasks in ASD, it is not clear if this brain irregularity persists during rest. If stronger connectivity of this pathway does exist at rest, it could indicate an intrinsic abnormality, and thus atypical socio-emotional processing even in the absence of direct social stimuli. Overconnectivity of this network could be reflective of social impairment in ASD. If individuals with ASD have abnormal reactions of this emotional circuit to social stimuli, it could detrimentally affect the way they behave toward others in social situations. The second objective of this study was to examine connectivity between the amygdala and the vmPFC during a socio-emotional task versus during rest, in adolescents with ASD and typically developing adolescents.

Hypotheses

Regarding the default network, the first research hypothesis was that ASD participants would show weaker functional connectivity between posterior and anterior default network structures in response to socio-emotional stimuli than control participants. Regarding the

amygdala-vmPFC pathway, the second research hypothesis was that the overconnectivity seen in ASD during socio-emotional processing would also appear during the resting state.

Method

Participants

A total of 21 children and adolescents with ASD and 35 healthy controls are included in this study. Of the 66 participants with ASD and 51 controls recruited, 45 ASD and 16 control participants were removed from all analyses due to movement greater than 2.5mm or incomplete fMRI scans resulting from discomfort. The default network analysis includes 21 participants with ASD and 30 controls. The included ASD participants consist of five females and sixteen males, and the included control participants consist of ten females and 20 males. The amygdala-vmPFC analysis includes fifteen participants with ASD and 35 controls. The included ASD participants consist of four females and eleven males, and the included control participants consist of nine females and 26 males.

Participants with ASD were recruited through the University of Michigan Autism and Communication Disorders Center. An ASD diagnosis (autism, Asperger's disorder, or pervasive developmental disorder not otherwise specified) was determined using the Autism Diagnostic Observation Schedule (Lord et al., 2000), the Autism Diagnostic Interview-Revised (Lord, Rutter, & Le Couteur, 1994), and clinical consensus (Lord et al., 2006). Control participants were recruited using flyers posted at community venues. Inclusion criteria consisted of a score of 85 or higher on either verbal or non-verbal cognitive functioning tests, a lack of orthodontic braces, and an age between nine and eighteen years. Controls were excluded if they had a neurologic or mental disorder. The Peabody Picture Vocabulary Test (PPVT; Dunn & Dunn, 1997) and the Ravens Progressive Matrices (Raven, 1960) were used to evaluate cognitive

functioning in controls. The Differential Ability Scales II – School Age (Elliott, 2005), the Stanford-Binet Intelligence Scales (Roid, 2003), and the Wechsler Intelligence Scale for Children IV (Wechsler, 2003) were given as cognitive measures to ASD participants.

Procedure

Data acquisition.

Resting. To collect data on functional connectivity during rest, a visual fixation cross (plus sign) was presented to each participant for 10 minutes in the scanner. Participants were instructed to let their minds wander and not think about anything in particular while looking at the cross. In order to correct for physiological noise due to respiratory and cardiac rhythms during data processing, physiological data were also collected during rest using the GE scanner, synchronized to the fMRI data. An abdominal pressure belt recorded each participant's respiratory rhythms, and a pulse oximeter was placed on each participant's left middle finger to record cardiac rhythms.

Socio-emotional task. Participants completed two 5-minute runs of a gender-recognition task with emotional faces during fMRI acquisition. The task utilized photographs of emotional (happy, sad, and fearful) and neutral faces. There were 30 trials of each emotion (happy, sad, and fearful), as well as neutral faces. Each trial began with the presentation of a fixation cross in the middle of the screen for 500ms, followed by the presentation of a face for 250ms. A blank screen then appeared for 1500ms, plus a jittered intertrial interval (ITI) ranging from 2s to 6s in order to obtain a better estimate of baseline. The gender-recognition task was used to monitor attention to the faces. Participants wore a response glove on their right hands, and were instructed to "push the button with your thumb if you see a male face, and with your pointer finger if you see a female face." They did so while the blank screen was displayed following each face. E-Prime

(Psychological Software Tools) was used to control the stimulus presentation and record the responses.

fMRI acquisition. Participants were scanned on a 3-Telsa GE Signa MRI scanner at the University of Michigan. For each participant, T_2*-weighted blood oxygen level dependent (BOLD) images were acquired using a reverse spiral sequence (Glover & Law, 2001; repetition time 2000ms, echo time 30ms, flip angle 90°, field of view 22cm, 64x64 matrix, 40 contiguous axial 3mm slices). Slices were acquired parallel to the anterior-posterior commissural line. A high-resolution 3D T1 axial overlay (TR-8.9, TE=1.8, flip angle=15°, FOV=26cm, 1.4mm slice thickness, 124 slices, 256x160 matrix) was collected for anatomical localization of the structural images. Additionally, a high-resolution SPGR image was acquired sagittally (flip angle 15°, FOV 26cm, 1.4mm slice thickness, 110 slices) to be used for co-registration of the resting functional images. An inversion-prepped T_1-weighted anatomic image using SPGR imaging (flip angle 15°, FOV 26cm, 1.4mm slice thickness, 110 sagittal slices) was also collected to facilitate normalization in functional images acquired during the faces task.

fMRI data analysis.

Data preprocessing. The fMRI data were preprocessed with the standard processing stream at the University of Michigan. First, outliers in the raw k-space data falling more than two standard deviations from the mean were replaced with the average of the neighboring time-points. Second, the k-space data were reconstructed to image space with a custom reconstruction program used for gridding and inverse 2D Fourier transform. To reduce artifacts from susceptibility regions, a field map correction was applied to the data. RETROICOR (Glover, Li, & Ress, 2000) was then used to remove noise due to respiratory and cardiac rhythms exclusively in the resting connectivity data, as resting data is more susceptible to this type of artifact. Next,

by phase-shifting and re-sampling the signal, images were corrected for differences in slice timing (Oppenheim, Schafer, & Buck, 1999). The middle slice was used as the temporal reference point. Finally, the MCFLIRT program in FMRIB Software Library (Jenkinson, Bannister, Brady, & Smith, 2002) was used to realign all images to the 10th functional image in order to correct for head motion.

Further preprocessing of the data was performed in the TaDLab using the SPM5 Matlab Toolbox (Wellcome Department of Cognitive Neurology, London, UK; http://www.fil.ion.ucl.ac.uk). High-resolution T1 anatomical images were co-registered to the functional images, and the images were then smoothed using an isotropic 8mm full width at half maximum (FWHM) Gaussian kernel. The time courses from each voxel were low-pass filtered with a 0.08Hz cutoff frequency, as resting state connectivity has previously been observed in this frequency band, and to exclude higher frequency sources of noise (Biswal, Yetkin, Haughton, & Hyde, 1995; Cordes et al., 2000).

Self-organizing map method for default network connectivity analysis. A self-organizing map algorithm was used to identify the posterior region of the default network in each individual participant, as previous papers have described (Peltier, Polk, & Noll, 2003; Wiggins et al., 2011). The timecourse of this posterior region, which includes the posterior cingulate cortex, precuneus, angular gyri, and inferior parietal lobule, was then averaged, and correlated with every other voxel in the participant's brain. This was done in order to calculate how functionally connected each part of the individual's brain is with the default network. The end product of these calculations is a correlation map, with a correlation value at every voxel of the brain, indicating how connected it is with the posterior region of the default network. The SOM method is advantageous because it uses an individualized reference to generate a connectivity map for

each participant instead of using a single, standardized seed for all participants. This data-driven method avoided seed placement bias for one group over another, and is advantageous for networks that cross anatomical boundaries, such as the default network. Because every participant had a correlation map, it was then possible to compare whether ASD or controls had stronger connectivity with the posterior hub.

Seed method for amygdala-vmPFC connectivity analysis. As the amygdala is clearly anatomically defined, we used the seed method of calculating connectivity for these analyses. In the seed method, images are normalized before preprocessing occurs. In order to reduce noise related to movement, a regression analysis was performed before generating functional connectivity maps by entering the 6 motion parameters as nuisance covariates for each subject. To create the functional connectivity maps, the data was run through in-house batch scripts in MATLAB (The Mathworks Inc. Natick, MA). Using these scripts, a seed region was placed in the laterobasal amygdala at MNI coordinates [28, -4, -22]. The laterobasal amygdala was chosen based on its role in social cognition and its relationship to childhood ASD (Kim et al., 2010). The specific seed region was based on Roy and colleagues' analysis of amygdala resting-state functional connectivity (2009) as well as previous data from the TaDLab on emotional face processing in ASD (Weng et al., 2010). The BOLD timecourses from the 4-voxel square around the seed were averaged to form a reference waveform, which was then correlated with all other voxels to generate a functional connectivity map for each participant.

Higher level analyses. The functional connectivity maps created by the SOM and seed methods were used in higher level analyses. For the default network and for the amygdala-vmPFC circuit, group-level random effects analyses were conducted in SPM5 to compare connectivity in ASD versus controls. This was done for the default network during the faces task,

and compared to previous published data from our lab (Wiggins et al., 2011) examining the default network during rest. A region of interest (ROI) analysis was used to examine functional connectivity between the posterior region of the default network and the frontal gyri. For the amygdala-vmPFC, the group-level analysis was performed during rest and during the faces task for comparison. ROI analyses focused on the vmPFC. Significance thresholds were small volume-corrected for multiple comparisons within each ROI using false discovery rate (FDR) correction (Genovese, Lazar, & Nichols, 2002).

Results

Faces Task Accuracy

The gender-recognition task was used to ensure that all participants were attending to the faces. While the average accuracy on the task was over 85% for both the ASD and control groups, an independent samples t-test revealed that there was a significant difference in accuracy between groups ($t(50) = 3.445$, $p = 0.001$), as shown in Table 1. This may indicate that ASD participants were less capable of discriminating between male and female faces as they appeared during the task, or that they were not attending as closely to the faces as the control participants were.

Cognitive Functioning Effects

An independent samples t-test was performed to determine whether or not there were group differences in either verbal or non-verbal cognitive functioning. Verbal IQ scores were obtained for all 35 control participants ($M = 113.9$, $SD = 14.4$) and all 21 ASD participants ($M = 105.7$, $SD = 17.2$). Non-verbal IQ scores were obtained for 33 of the control participants ($M = 103.9$, $SD = 11.5$) and 20 of the ASD participants ($M = 90.0$, $SD = 18.2$). While the control group scored slightly higher on both cognitive measures, the groups did not significantly differ in either

verbal ($t(54) = 1.926$, $p = 0.059$) or non-verbal ($t(51) = 1.204$, $p = 0.234$) cognitive functioning, as shown in Table 2.

Default Network

Both the ASD and control groups showed functional connectivity of the default network during the faces task (Table 3). The first hypothesis was that the ASD group would have weaker functional connectivity between posterior and anterior default network structures in response to socio-emotional stimuli than the control group. Addressing this, while the analysis did not quite pass a correction for multiple comparisons, there was a trend of underconnectivity in ASD during the faces task. Most notably, ASD participants showed weaker connectivity between the SOM-identified posterior hub of the default network and a cluster in the left superior frontal gyrus (lSFG) (xyz = -24, 52, -4; $t(49) = 2.89$, $p = .060$ small volume corrected for left superior frontal orbital cortex using FDR). During rest, our lab previously found that ASD participants showed weaker connectivity between the SOM-identified posterior hub of the default network and the right SFG (xyz = 22, 58, 12; $t(78) = 3.91$; $p = .037$ small volume corrected for the right superior frontal gyrus using FWE) (Wiggins et al., 2011). Thus, compared to the default network during rest (Wiggins et al., 2011), there was a trend of underconnectivity of the same structure, albeit in the contralateral hemisphere, during socio-emotional processing. Functional connectivity values from a 4mm radius sphere around this lSFG cluster were extracted and averaged for comparison across task conditions. An independent samples t-test revealed a significant difference in functional connectivity to the lSFG between task conditions in the ASD group ($t(36) = 2.255$, $p = 0.030$), but not in the control group ($t(57) = -0.826$, $p = 0.412$), as shown in Table 4. Figure 1 illustrates these results.

There was an overall pattern of weaker default network connectivity in the ASD group than in the control group during the faces task (Table 3), but direct comparison in SPM5 did not yield significant group differences. New analysis of previously collected data showed similar patterns of weaker connectivity in the ASD group during rest (Table 5). There was also an overall pattern of weaker functional connectivity between the posterior default network and other default network structures in the ASD group than in the control group during the faces task (Table 6), but direct comparison in SPM5 did not yield significant group differences.

Amygdala-vmPFC

Due to a series of technical difficulties and time constraints, we are unable to report on results for the analysis of amygdala-vmPFC connectivity at this time.

Discussion

The goal of this study was to enhance understanding of networks of brain connectivity in relation to ASD. Specifically, the default network and the amygdala-vmPFC pathway were the foci of investigation. For default network analysis, we used a self-organizing map algorithm to obtain individualized correlation maps for each participant, identifying the posterior hub of the default network as a reference to calculate connectivity for each individual. For the amygdala-vmPFC analysis, a seed region in the laterobasal amygdala was chosen based on previous research (Roy et al., 2009; Weng et al., 2010) to be used as a reference to generate correlation values with ROIs in the vmPFC.

The first research hypothesis was that ASD participants would show weaker functional connectivity between posterior and anterior default network structures in response to socio-emotional stimuli than control participants, as was previously observed during the resting state. This hypothesis was not confirmed by the data, but there was a trend of underconnectivity in the

ASD group, suggesting there may be a modest effect if analyzed with a larger sample. The second research hypothesis was that that the overconnectivity seen in ASD during socio-emotional processing would also appear during the resting state. Due to technical limitations during second-level analyses, it is still unclear whether or not this hypothesis was supported by the data.

Implications

Default network. A similar pattern of underconnectivity between posterior and anterior default network structures as was previously seen during rest was found to persist during socio-emotional processing. This is may indicate atypical functioning of default network structures. During rest, it was possible that the weaker connectivity found in the default network was a function of what the ASD versus control participants were thinking about when told to "let their minds wander." For example, if the control group thought about social interactions during the resting task and the ASD group did not, this could explain the observed differences in default network engagement. However, as both groups were required to attend to the socio-emotional stimuli during the faces task, differences in functional connectivity could be explained by intrinsically altered default network functioning. Dysfunction of social processing pathways in ASD also poses an explanation for the significantly weaker engagement of the lSFG during the faces task than during rest that was observed (Table 6; Figure 1). However, it is interesting to note that significant differences between the ASD and control groups were previously found at rest, but only a trend was observed during the task. An alternative explanation could be that locking all participants into a task might normalize the default network activation. In keeping with this interpretation, the trend of underconnectivity found in the ASD group might then be explained by the level of difficulty of the task for each group. The gender-identification task may

be more challenging for participants with ASD than for control participants, resulting in slightly decreased default network connectivity due to less attention to the socio-emotional aspects of the faces.

Amygdala-vmPFC. The second research hypothesis was that the overconnectivity observed between the amygdala and ventromedial prefrontal cortex during socio-emotional processing in ASD would persist during rest. Had we been able to complete analysis and found that the hypothesis was supported, it would indicate intrinsic dysfunction of this pathway. This would signify atypical socio-emotional processing even in the absence of direct social stimuli, potentially reflecting and/or exacerbating the social impairment characteristic of ASD.

Limitations

This study has multiple limitations. First, there was a high attrition rate in this study, specifically of the ASD group. Therefore, the analyses may not include a representative sample.

Second, artifacts due to head movement and/or physiological noise could detrimentally affect the analyses. To control for head motion artifact, all functional images were realigned, and scans containing movement greater than 2.5mm in the x, y, or z direction were excluded from analysis. To control for physiological noise, correction was completed based on cardiac and respiratory recordings for each participant.

Third, control participants performed more accurately on the gender recognition faces task than did ASD participants. This may be due to participants with ASD paying less attention to the faces as they were presented during fMRI acquisition. If this is so, lack of attention to the social stimuli may be affecting the results.

Fourth, several participant factors may confound the results. These include age, medication effects, and cognitive functioning effects. Because participants ranged in age from

nine to eighteen, it is possible that age-related differences could account for, or mask, some of the results. Additionally, nine of the 21 participants with ASD received psychotropic medication. However, previous studies have found that medication does not drive connectivity effects (Monk et al., 2009; Weng et al., 2010; Wiggins et al., 2011). Finally, control participants performed slightly better on the cognitive measures than ASD participants. However, as there were no significant differences between groups in either the verbal or the non-verbal domains, it is unlikely that cognitive functioning effects are driving the results.

Future Directions

The present study brings to light several possibilities for future research on functional connectivity and ASD. First and foremost, analysis of amygdala-vmPFC connectivity during rest should be completed and compared between the ASD and control groups, as well as compared to connectivity during the faces task. Second, as SOM allows for more precise analysis due to its individualized nature, future studies could employ this method for amygdala-vmPFC analysis in addition to default network analysis. Third, age-related effects could be further investigated to gain insight into the developmental trajectory of the default network and the amygdala-vmPFC network in multiple task contexts in ASD versus typically developing individuals. This type of analysis has recently begun for the default network (Wiggins et al., 2011), but not yet for amygdalar networks. Fourth, as the correlation between default network connectivity and symptom severity has begun to be investigated (Monk et al., 2009; Weng et al., 2010), future studies could look into a correlation between ASD symptom severity and amygdala-vmPFC connectivity. Fifth, future research could directly examine the idea that the task condition might be normalizing default network activation in ASD. Finally, findings from the present study could be used to further investigate genetic links to the brain abnormalities found in ASD.

References

APA. (1994). *Diagnostic and statistical manual of mental disorders* (4th ed.). Washington, DC: American Psychiatric Association.

Ashwin, C., Baron-Cohen, S., Wheelwright, S., O'Riordan, M., & Bullmore, E. T. (2007). Differential activation of the amygdala and the 'social brain' during fearful face-processing in asperger syndrome. *Neuropsychologia, 45,* 2–14.

Baron-Cohen, S., Ring, H., Moriarty, J. Schmitz, B., Costa, D., & Ell, P. (1994). Recognition of mental state terms: Clinical findings in children with autism and a functional neuroimaging study of normal adults. *The British Journal of Psychiatry, 165*, 640-649.

Belmonte, M. K., Allen, G., Beckel-Mitchener, A., Boulanger, L. M., Carper, R. A. & Webb, S. J. (2004). Autism and abnormal development of brain connectivity. *The Journal of Neuroscience, 24*, 9228-9231.

Biswal, B., Yetkin, F. Z., Haughton, V. M., & Hyde, J. S. (1995). Functional connectivity in the motor cortex of resting human brain using echo-planar MRI. *Magnetic Resonance in Medicine. 34*, 537-41.

Buckner, R. L., Andrews-Hanna, J. R., & Schacter, D. L. (2008). The brain's default network: Anatomy, function, and relevance to disease. *Annals of the New York Academy of Sciences, 1124*, 1-38.

Buckner, R. L., & Carroll, D. C. (2007). Self-projection and the brain. *Trends in Cognitive Sciences, 11*, 49-57.

Cordes, D., Haughton, V. M., Arfanakis, K., Wendt, G. J., Turski, P. A., Moritz, C. H., … & Meyerand, M. E. (2000). Mapping functionally related regions of brain with functional connectivity MR imaging. *American Journal of Neuroradiology, 21*, 1636-44.

Dunn, L. M., & Dunn, L. M. (1997). *Peabody Picture Vocabulary Test - Revised Manual*. Circle Pines, MN: American Guidance Services.

Elliott, C. D. (2005). *The differential ability scale* (2nd ed.). In D. P. Flanagan & P. L. Harrison (Eds.), *Contemporary intellectual assessment: Theories, tests, and issues*. New York: Guilford Press.

Fox, M. D., Snyder, A. Z., Vincent, J. L., Corbetta, M., Van Essen, D. C., & Raichle, M. E. (2005). The human brain is intrinsically organized into dynamic, anticorrelated functional networks. *Proceedings of the National Academy of Sciences of the United States of America, 102*, 9673-9678.

Friston, K. J., Frith, C. D., Liddle, P. F., & Frackowiak, R. S. J. (1993). Functional connectivity: The principal component analysis of large (PET) data sets. *Journal of Cerebral Blood Flow & Metabolism, 13*, 5-14.

Frith, U., & Frith, C. D. (2003). Development and neurophysiology of mentalizing. *Philosophical Transactions of the Royal Society of London Series B: Biological Sciences, 358*, 459-473.

Genovese, C. R., Lazar, N. A., & Nichols, T. (2002). Thresholding of statistical maps in functional neuroimaging using the false discovery rate. *Neuroimage, 15*, 870-878.

Glover, G. H., Li, T. Q., & Ress, D. (2000). Image-based method for retrospective correction of physiological motion effects in fMRI: RETROICOR. *Magnetic Resonance in Medicine, 44*, 162-167.

Glover, G. H., & Law, C. S. (2001). Spiral-in/out BOLD fMRI for increased SNR and reduced susceptibility artifacts. *Magnetic Resonance in Medicine, 46*, 515-22.

Greicius, M. D., Krasnow, B., Reiss, A. L., & Menon, V. (2003). Functional connectivity in the

resting brain: a network analysis of the default mode hypothesis. *Proceedings of the National Academy of Sciences of the United States of America, 100*, 253-8.

Gusnard, D. A., & Raichle, M. E. (2001). Searching for a baseline: Functional imaging and the resting human brain. *Nature Reviews Neuroscience, 2*, 685-694.

Hadjikhani, N., Joseph, R. M., Snyder, J., & Tager-Flusberg, H. (2007). Abnormal activation of the social brain during face perception in autism. *Human Brain Mapping, 28*, 441–449.

Jenkinson, M., Bannister, P., Brady, M., & Smith, S. (2002). Improved optimization for the robust and accurate linear registration and motion correction of brain images. *Neuroimage, 17*, 825-41.

Kim, J. E., Lyoo, I. K., Estes, A. M., Renshaw, P. F., Shaw, D. W., Friedman, S. D., … & Dager, S.R. (2010). Laterobasal amygdalar enlargement in 6- to 7-year-old children with autism spectrum disorders. *Archives of General Psychiatry, 67*, 1187-1197.

Lord, C., Rutter, M., & Le Couteur, A. (1994). Autism Diagnostic Interview-Revised: a revised version of a diagnostic interview for caregivers of individuals with possible pervasive developmental disorders. *Journal of Autism and Developmental Disorders, 24*, 659-85.

Lord, C., Risi, S., Lambrecht, L., Cook, E. H. J., Leventhal, B. L., DiLavore, P. C., … & Rutter, M. (2000). The autism diagnostic observation schedule-generic: A standard measure of social and communication deficits associated with the spectrum of autism. *Journal of Autism and Developmental Disorders, 30*, 205-23.

Lord, C., Risi, S., DiLavore, P. S., Shulman, C., Thurm, A., & Pickles, A. (2006). Autism from 2 to 9 years of age. *Archives of General Psychiatry, 63*, 694-701.

Monk, C. S., Peltier, S. J., Wiggins, J. L., Weng, S. J., Carrasco, M., Risi, S., & Lord, C. (2009).

Abnormalities of intrinsic functional connectivity in autism spectrum disorders. *Neuroimage, 47*, 764-72.

Monk, C. S., Weng, S. J., Wiggins, J. L., Kurapati, N., Louro, H. M., Carrasco, M., … & Lord, C. (2010). Neural circuitry of emotional face processing in autism spectrum disorders. *Journal of Psychiatry & Neuroscience, 35*, 105-114.

Oppenheim, A. V., Schafer, R. W., & Buck, J. R. (1999). *Discrete-time signal processing* (2nd ed.). Upper Saddle River, NJ: Prentice Hall.

Peltier, S. J., Polk, T. A., & Noll, D. C. (2003). Detecting low-frequency functional connectivity in fMRI using a self-organizing map (SOM) algorithm. *Human Brain Mapping, 20*, 220-226.

Raven, J. C. (1960). *Guide to using the standard progressive matrices*. London, UK: Lewis.

Roid, G. H. (2003). *Stanford-Binet intelligence scales: Examiner's manual* (5th ed.). Itasca, IL: Riverside Publishing.

Roy, A. K., Shehzad, Z., Margulies, D. S., Kelly, A. M., Uddin, L. Q., Gotimer, K., … & Milham, M. P. (2009). Functional connectivity of the human amygdala using resting state fMRI. *Neuroimage, 45*, 614-626.

Wechsler, D. (2003). *Wechsler intelligence scale for children* (4th ed.). San Antonio, TX: Harcourt Assessment.

Weng, S. J., Wiggins, J. L., Peltier, S. J., Carrasco, M., Risi, S., Lord, C., & Monk, C. S. (2010). Alterations of resting state functional connectivity in the default network in adolescents with autism spectrum disorders. *Brain Research, 1313*, 202-214.

Weng, S. J., Carrasco, M., Swartz, J. R., Wiggins, J. L., Kurapati, N., Liberzon, I., … & Monk, C.

S. (2011). Neural activation to emotional faces in adolescents with autism spectrum disorders. *Journal of Child Psychology and Psychiatry, 52*, 296-305.

Wiggins, J. L., Peltier, S. J., Ashinoff, S., Weng, S. J., Carrasco, M., Welsh, R. C., … & Monk, C. S. (2011). Using a self-organizing map algorithm to detect age-related changes in functional connectivity during rest in autism spectrum disorders. *Brain Research, 1380*, 187-197.

Author Note

Samantha Ashinoff, Department of Psychology, University of Michigan, Ann Arbor.

Many thanks to my mentor, Dr. Christopher Monk, for working with me on this project. He was a great advisor, and I learned so much working in his Translational and Developmental Neuroscience Laboratory. I also thank Jillian Lee Wiggins for all of her invaluable help and support at every stage of this project. As always, special thanks to Mom and Dad.

Table 1

Faces Task Accuracy

	Independent Samples t-Test					
	Mean Difference	t	df	p	95% Confidence Interval of the Difference Lower	Upper
Overall	0.098	3.445	50	0.001	0.041	0.155

Table 2

Cognitive Functioning

	Independent Samples t-Test					
	Mean Difference	t	df	p	95% Confidence Interval of the Difference Lower	Upper
VIQ	8.248	1.926	54	0.059	-0.339	16.834
NVIQ	4.909	1.204	51	0.234	-3.274	13.092

Table 3

Posterior Default Network Connectivity During Socio-Emotional Processing

(A) ASD group

Region	Cluster Size	T *df* = 49	$P_{FDR\text{-}corr}$	MNI Coordinates x	y	z
L posterior cingulate	408	3.29	0.017	-6	-60	24
	2	2.37	0.020	-10	-44	8
R posterior cingulate	433	3.74	0.005	10	-58	16
L precuneus	1064	3.65	0.028	-2	-50	30
R precuneus	184	4.34	0.014	34	-86	32
	1388	4.04	0.014	6	-50	32
	8	2.94	0.027	26	-84	24
L angular gyrus	143	2.99	0.062	-48	-62	30
R angular gyrus	321	3.99	0.005	50	-70	30
L inferior parietal lobule	180	2.63	0.392	-46	-62	38
R inferior parietal lobule	142	3.42	0.339	44	-72	38

(B) Control group

Region	Cluster Size	T *df* = 49	$P_{FDR\text{-}corr}$	MNI Coordinates x	y	z
L posterior cingulate	440	9.58	<0.001	-4	-58	24
	2	4.78	<0.001	-10	-44	8
R posterior cingulate	450	10.09	<0.001	6	-54	24
L precuneus	2186	10.45	<0.001	-4	-50	30
	10	2.15	0.030	-22	-84	24
R precuneus	2197	10.34	<0.001	6	-52	30
L angular gyrus	272	8.04	<0.001	-48	-62	30
R angular gyrus	370	7.25	<0.001	44	-70	36
L inferior parietal lobule	516	7.26	<0.001	-50	-56	38
	118	4.51	<0.001	-46	-50	24
R inferior parietal lobule	345	7.48	<0.001	44	-72	38
	184	3.38	0.011	46	-50	24

Note. Functional connectivity within the SOM-identified posterior hub of the default network during socio-emotional processing, indicating default network activation during the faces task. The table shows peak voxels. L= left, R = right.

Table 4

lSFG Connectivity Differences

	Independent Samples t-Test					
	Mean Difference	t	df	p	95% Confidence Interval of the Difference Lower	Upper
ASD	198.029	2.255	36	0.030	19.026	359.031
Control	-49.102	-0.826	57	0.412	-168.088	69.885

Note. Differences in activation of the lSFG functional ROI (xyz = -24, 52, -4) between conditions (rest versus faces task) in each group.

Table 5

Posterior Default Network Connectivity During Rest

(A) ASD

Region	Cluster Size	T *df* = 78	$P_{FDR\text{-}corr}$	MNI Coordinates x	y	z
L posterior cingulate	587	3.93	0.010	-2	-32	26
R posterior cingulate	428	3.62	0.047	4	-32	26
L precuneus	1478	5.07	0.002	-10	-44	52
R precuneus	788	3.58	0.099	2	-50	30
L angular gyrus	225	3.55	0.016	-48	-58	36
R angular gyrus	60	2.29	0.203	46	-72	30
L inferior parietal lobule	1175	4.17	0.015	-42	-54	38
	105	3.48	0.015	-40	-24	30
R inferior parietal lobule	201	2.84	0.454	54	-52	40

(B) Controls

Region	Cluster Size	T *df* = 78	$P_{FDR\text{-}corr}$	MNI Coordinates x	y	z
L posterior cingulate	784	9.36	<0.001	-6	-62	22
R posterior cingulate	829	10.09	<0.001	8	-46	24
L precuneus	2079	9.53	<0.001	-4	-66	36
	178	6.20	<0.001	-42	-72	34
R precuneus	2353	10.15	<0.001	6	-50	30
	108	5.28	<0.001	42	-68	34
L angular gyrus	320	7.36	<0.001	-46	-58	36
R angular gyrus	325	7.51	<0.001	50	-62	30
L inferior parietal lobule	719	7.42	<0.001	-44	-58	38
	100	5.26	<0.001	-48	-50	24
R inferior parietal lobule	448	6.10	<0.001	52	-58	38
	179	5.85	<0.001	44	-50	22

Note. Functional connectivity within the SOM-identified posterior hub of the default network during rest. New analysis of data from previous research in the lab (Wiggins et al., 2011). The table shows peak voxels. L= left, R = right.

Table 6

Default Network Connectivity During Socio-Emotional Processing

(A) ASD group

Region	Cluster Size	T *df* = 49	$P_{FDR\text{-}corr}$	MNI Coordinates x	y	z
L superior frontal gyrus	12	2.33	0.598	-2	60	2
R superior frontal gyrus	4	3.67	0.091	18	34	34
Medial frontal gyrus	778	3.72	0.116	16	34	36
	74	2.46	0.132	-14	-24	60
	118	2.34	0.132	-4	60	0
Bilateral anterior cingulate	401	4.69	0.011	16	18	28

(B) Control group

Region	Cluster Size	T *df* = 49	$P_{FDR\text{-}corr}$	MNI Coordinates x	y	z
L superior frontal gyrus	12	5.03	<0.001	-6	60	-6
	21	4.66	0.001	-4	58	2
	43	4.64	0.001	-14	46	22
R superior frontal gyrus	18	4.62	0.004	4	60	2
	4	4.04	0.005	18	34	34
	13	4.00	0.005	4	60	-6
Medial frontal gyrus	254	5.98	<0.001	-6	52	-8
	1343	5.83	<0.001	-8	46	24
	209	5.26	<0.001	2	54	-4
	157	3.67	0.001	-6	-30	56
Bilateral anterior cingulate	2126	5.24	<0.001	-6	48	-4

Note. Functional connectivity between the SOM-identified posterior hub of the default network and other default network structures during the faces task. The table shows peak voxels. L= left, R = right.

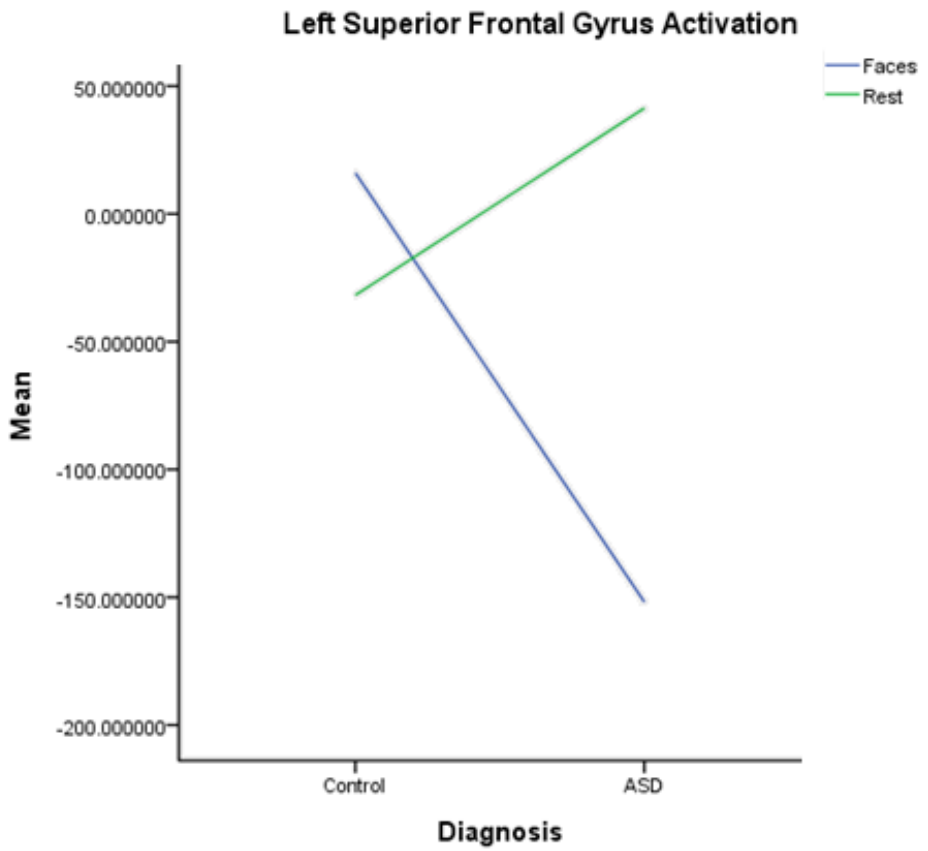

Figure 1. Differential activation of the lSFG functional ROI (peak voxel at xyz = -24, 52, -4). To depict connectivity for each subject, z values were extracted from a sphere with a radius of 4mm around the peak. Means for the ASD and control groups are shown in the graph.